Author Manuscript

Author Manuscript

Author Manuscript

Author Manuscript

HHS Public Access

Author manuscript

Cell Stem Cell. Author manuscript; available in PMC 2024 May 04.

Published in final edited form as:

Cell Stem Cell. 2023 May 04; 30(5): 665–676.e4. doi:10.1016/j.stem.2023.04.007.

IGFBP2 expressing midlobular hepatocytes preferentially contribute to liver homeostasis and regeneration

Yu-Hsuan Lin[1], **Yonglong Wei**[1], **Qiyu Zeng**[1], **Yunguan Wang**[2], **Chase A. Pagani**[1], **Lin Li**[1], **Min Zhu**[1], **Zixi Wang**[1], **Meng-Hsiung Hsieh**[1], **Natasha Corbitt**[1], **Yu Zhang**[1], **Tripti Sharma**[1], **Tao Wang**[2], **Hao Zhu**[1,*]

[1]Children's Research Institute, Departments of Pediatrics and Internal Medicine, Center for Regenerative Science and Medicine, University of Texas Southwestern Medical Center, Dallas, TX 75390, USA.

[2]Quantitative Biomedical Research Center, Department of Population and Data Sciences, Center for the Genetics of Host Defense, University of Texas Southwestern Medical Center, Dallas, TX, 75390, USA.

Summary

While midlobular hepatocytes in zone 2 are a recently identified cellular source for liver homeostasis and regeneration, these cells have not been exclusively fate mapped. We generated a *Igfbp2-CreER* knockin strain, which specifically labels midlobular hepatocytes. During homeostasis over 1 year, zone 2 hepatocytes increased in abundance from occupying 21% to 41% of the lobular area. After either pericentral injury with carbon tetrachloride or periportal injury with DDC, IGFBP2+ cells replenished lost hepatocytes in zones 3 and 1, respectively. IGFBP2+ cells also preferentially contributed to regeneration after 70% partial hepatectomy, as well as liver growth during pregnancy. Because IGFBP2 labeling increased substantially with fasting, we used single nuclear transcriptomics to explore zonation as a function of nutrition, revealing that the zonal division of labor shifts dramatically with fasting. These studies demonstrate the contribution of IGFBP2-labeled zone 2 hepatocytes to liver homeostasis and regeneration.

eTOC statement

The liver consists of different zones with spatial heterogeneity in their metabolic functions. Here, a new *Igfbp2-CreER* line, which enabled direct tracing of midlobular hepatocytes, showed that IGFBP2+ cells serve as a source of new hepatocytes during normal homeostasis and regeneration.

[*]**Correspondence and lead contact:** Hao Zhu, Hao.Zhu@utsouthwestern.edu, Phone: (214) 648-2850.

Author contributions

Y.H.L. and H.Z. conceived the project, performed the experiments, and wrote the manuscript. Y.W. analyzed the mouse models and performed animal experiments. Q.Z. assisted with the immunostaining. Y.W., C.A.P. and T.W. performed bioinformatic analysis for the snRNA-seq. M.Z. performed the transplantation surgery. M.Z. and Z.W. generated the scRNA-seq data. M.H.H. assisted with animal experiments and mice husbandry. N.C. provided human liver samples. Y.Z. and T.S. generated the *Igfbp2-CreER* transgenic mouse.

Declaration of Interests

These interests are not directly related to the contents of this paper.

Publisher's Disclaimer: This is a PDF file of an unedited manuscript that has been accepted for publication. As a service to our customers we are providing this early version of the manuscript. The manuscript will undergo copyediting, typesetting, and review of the resulting proof before it is published in its final form. Please note that during the production process errors may be discovered which could affect the content, and all legal disclaimers that apply to the journal pertain.

Author Manuscript Author Manuscript Author Manuscript Author Manuscript

Abstract

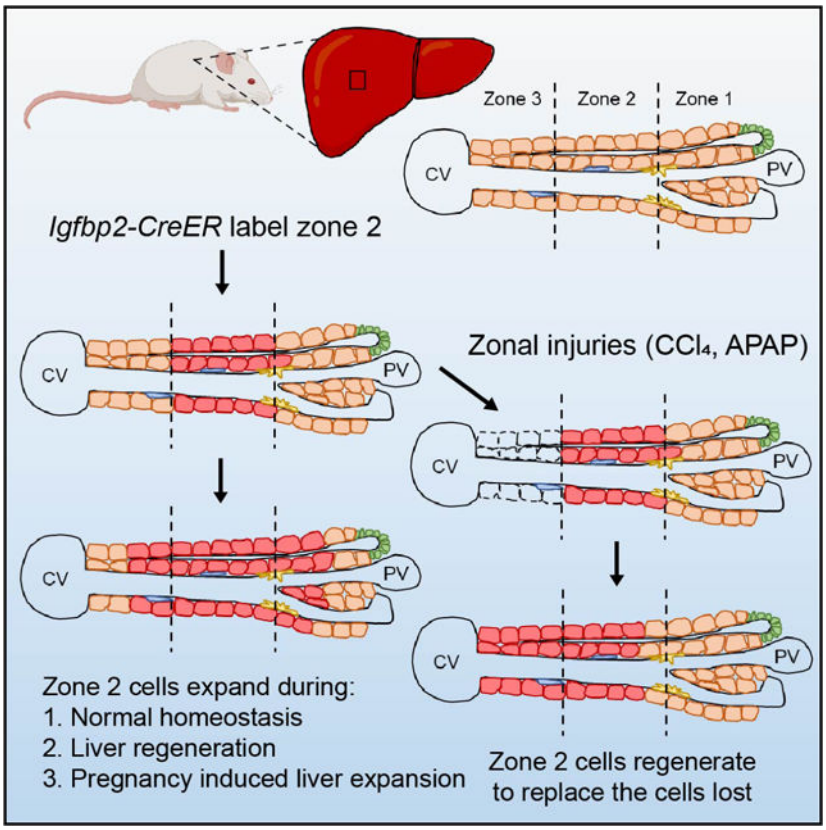

Introduction

The source of new liver cells during homeostasis and regeneration has been intensely debated. Many studies have proposed diverse cell types as liver stem cells: Sox9 expressing cells near the portal triad [1,2]; Axin2 expressing hepatocytes near the central vein [3]; Tert expressing hepatocytes distributed throughout the lobule [4]. Other studies have come to different conclusions [5,6]. As single cell technologies were being applied to the liver, metabolic zonation emerged as an important source of cellular heterogeneity [7]. To determine whether this zonal heterogeneity leads to differences in regenerative capacity, we previously compared the contraction and expansion of different zonal compartments using 14 orthogonal *CreER* mouse strains. Using these tools, we and others showed that zone 2 cells are a major source of new hepatocytes during liver growth, maintenance, and tissue repair [6,8,9].

While midlobular hepatocytes in zone 2 are a potential source of new hepatocytes, there are still major questions and unresolved controversies. Prior studies, including ours, used negative tracing approaches to generate support for zone 2 expansion. Because zone 2 cells are ill-defined and do not have a singular genetic marker, these studies were unable to exclusively trace zone 2 cells. For example, we used *Hamp2*, which is enriched in zone 2, to probe this population. However, *Hamp2* is also expressed in some zone 1 and 3 cells.

Author Manuscript Author Manuscript Author Manuscript Author Manuscript

Other studies using pan-zonal AAV-TBG-Cre and Ki67-CreER tracing tools faced similar caveats [6,9]. In this study, we focused on a maker that is more restricted to zone 2 cells. We generated a *Igfbp2-CreER* knockin strain that specifically labels midlobular hepatocytes. Our study of the IGFBP2+ population again showed that zone 2 populations preferentially contribute to homeostatic repopulation of the liver over long time periods. In addition, our studies comparing IGFBP2 to other markers such as HAMP2 suggest heterogeneity among different zone 2 populations.

Because there were previously no exclusive tracing markers for zone 2, there was no high fidelity method to assess zone 2's contribution to diverse regenerative processes. Here, we used the *Igfbp2* tracer to independently assess the contribution of zone 2 cells in both commonly and poorly studied injury assays. Our results provided direct evidence that midlobular cells regenerate after zone 1 and 3 injuries caused by liver toxins. In addition, we quantified how much zone 2 cells contribute to 1) partial hepatectomy induced regeneration, 2) hepatocyte transplant induced repopulation of a chronic liver disease model, and 3) a profound but rarely studied process - pregnancy induced liver enlargement. Remarkably, the preferential contribution from zone 2 was observed in each of these models.

Results

Igfbp2-CreER mice efficiently label midlobular hepatocytes

Using CRISPR genome editing, we created a new *Igfbp2-CreER* strain in which the IRES cassette followed by *CreERT2* (hereafter *CreER*) recombinase was integrated into the endogenous 3' untranslated region (3'UTRs) of *Igfbp2* (Figure 1A). By crossing *Igfbp2-CreER* and *Rosa-LSL-tdTomato* reporter mice, we generated lineage tracing mice with permanent Tomato protein expression in IGFBP2+ hepatocytes after tamoxifen administration (Figure 1B,C and Figure S1A,B). We used an IGFBP2 antibody to perform immunofluorescence staining in the *Igfbp2-CreER; LSL-tdTomato* labeled liver. Although the percentage of Tomato+ cells was less than the percentage of endogenous IGFBP2 expressing cells, Tomato and IGFBP2 expression were largely overlapping (Figure S1C). Therefore, the *Igfbp2-CreER* strain labels zone 2 hepatocytes that express endogenous IGFBP2. There was very little reporter activation (less than 0.1% of cells) when oil alone as a vehicle was given, and this rare population did not significantly contribute to homeostasis after 26-weeks of tracing (Figure S1D). We quantified the distribution of Tomato+ cells across all zones and found that it was highest in the midlobule, or zone 2 (Figure 1D). Almost no Glutamine Synthetase (GS)+ cells in zone 3 of the lobule were labeled by Tomato. Occasional cells adjacent to the portal trials were labeled, but the labeling in this zone 1 region was much more sparse than in zone 2. Tomato+ cells were located on the border of the periportal region as defined by E-cadherin, with around half of the Tomato+ cells expressing E-cadherin (Figure S1E).

Igfbp2 expression is known to be nutritionally regulated, as hepatic *Igfbp2* mRNA increases after fasting [10]. To examine whether Cre mediated labeling efficiency was also nutritionally controlled, mice were given tamoxifen at noon after overnight fasting (Figure 1B–C). To exclude the potential impact from circadian regulation, control mice that were fed normally were also given tamoxifen at noon. Compared to fed mice given tamoxifen in the evening

Author Manuscript Author Manuscript Author Manuscript Author Manuscript

or fed mice given tamoxifen at noon (20.79 ± 9.75% and 20.2 ± 5.47% (mean ± SD) respectively), overnight fasted mice had a large increase in Tomato labeling (28.90 ± 5.93%) (Figure 1E). The fasted group also had reduced variability in Tomato labeling than the fed group given tamoxifen in the evening.

Genomic *CreER* integration can cause unexpected biological effects that can influence hepatocyte turnover and long-term lineage tracing results. To confirm that the *Igfbp2-CreER* transgene did not influence hepatocyte turnover, we gave the mice 5-ethynyl-2′-deoxyuridine (EdU) in the drinking water for 10 days (Figure S2A). The frequency and spatial distribution of EdU+ hepatocytes were quantified as previously described [4]. Compared to wild-type (WT) livers, *Igfbp2-CreER* knockin mice exhibited a similar EdU distribution, with zone 2 having the highest frequency of proliferating cells (Figure S2B). Collectively, these results showed that the *Igfbp2-CreER* strain can efficiently label midlobular hepatocytes to different extents with the evening or fasting tamoxifen approach. Furthermore, there was no evidence that this strain caused significant ectopic labeling or artificially favored clonal expansion from any particular zone.

Midlobular zone 2 cells marked by *Igfbp2* expand during normal homeostasis

We previously used distinct *CreER* lines to label different zonal compartments and systematically compared the contraction and expansion of different hepatocytes subpopulations [8]. The results revealed that zone 2 hepatocytes are the major source for renewal during normal homeostasis. Sparsely labeled zone 2 hepatocytes by *Hamp2-CreER* (7.4 ± 0.7% of the slide area was labeled) showed clonal expansion after 12 months of tracing (27.4 ± 4.1%) [8]. To determine if the expansion was only applicable to the rare subpopulation labeled by HAMP2, we employed the *Igfbp2-CreER* line for lineage tracing under steady-state homeostatic conditions. Fed mice were given tamoxifen in the evening and traced for 2, 12, 26, and 52 weeks (Figure 2 and Figure S3A). The images from all timepoints exhibited a similar zonated pattern of Tomato distribution, indicating that there was no replacement of unlabeled populations from either zone 1 or zone 3 (Figure 2B and Figure S3B). To evaluate whether labeled zone 2 cells increased in number during homeostasis, we measured the area occupied by Tomato+ cells over 12-, 26- and 52-week periods. In the evening tamoxifen group, the Tomato labeled area went from 20.79 ± 9.75% (2 weeks post-tamoxifen) to 31.13 ± 14.47% (12 weeks), 34.79 ± 14.63% (26 weeks), and 40.71 ± 14.96% (52 weeks) (Figure 2C).

Because zone 2 has been defined differently in various studies, the extent to which midlobular populations expand is dependent on the size of the zone 2 population labeled initially. We reasoned that increasing the initially labeled size of the zone 2 domain would lead to a reduction in the relative expansion over time. To label and trace a broader midlobular population, we performed the homeostasis tracing experiments using tamoxifen labeling under fasting conditions. Similar spatial distributions of Tomato+ cells were observed over 2, 12 and 26 weeks (Figure S4A–S4C). We noticed an increase of Tomato area from 28.90 ± 5.93% (2 weeks) to 35.26 ± 12.32% (12 weeks) and 37.27 ± 10.05% (26 weeks) after fasting tamoxifen labeling (Figure S4D). Compared to evening tamoxifen, the change in Tomato+ area was lower in the fasting labeled group. This suggested that

Author Manuscript Author Manuscript Author Manuscript Author Manuscript

some of the additionally labeled cells near the PV likely did not contribute to the expansion, since the final Tomato labeling result was similar. Overall, we found that midlobular zone 2 hepatocytes labeled by the *Igfbp2-CreER* strain expanded during homeostasis.

IGFBP2 expressing zone 2 cells contribute to regeneration after zone 1 and 3 injuries

To determine whether zone 2 cells labeled using *Igfbp2-CreER* mice contribute to regeneration after common liver injuries, we challenged mice with toxins that damage hepatocytes in zone 1 and 3 (Figure 3A,B). In these experiments, we used the fasting tamoxifen approach to increase the consistency of labeling before various injuries. After tamoxifen labeling, we injected mice with either single doses of carbon tetrachloride (CCl_4) or acetaminophen (APAP) to cause centrilobular hepatic necrosis. After two weeks, the necrotic areas fully recovered and were replaced by the remaining adjacent hepatocytes. Tomato+ cells shifted from the midlobular to centrilobular regions, even coexpressing Tomato and GS, indicating that proliferating zone 2 hepatocytes regenerated to replace the cells lost in zone 3 (Figure 3C). The percentage of Tomato labeling was 50.24 ± 9.95% and 49.52 ± 10.57% after one dose CCl_4 or APAP, compared to non-injured control mice (32.75 ± 6.16%) (Figure 3D). To investigate a cholestatic injury focused on the opposite end of the lobule, we fed mice with 0.1% 3,5-diethoxycarbonyl-1,4-dihydrocollidine (DDC) for 4 weeks. Chronic DDC feeding increases biliary porphyrin secretion and induces ductular reaction, modeling human cholangiopathies such as primary sclerosing cholangitis, primary biliary cirrhosis, and drug-induced bile duct damage [11]. After DDC, biliary damage was associated with ductular reactions in periportal regions, which were surrounded by Tomato+ cells (Figure 3E). To allow the recovery and regeneration of hepatocytes, we discontinued DDC for two weeks. After this washout period, the periportal area was filled with Tomato+ cells (Figure 3E). The Tomato+ area was 39.44 ± 6.07% in DDC fed mice, compared to non-injured control mice (33.45 ± 3.73%) and to injured mice before washout (31.58 ± 2.62%) (Figure 3F). Since a majority of liver injuries cause damage in zone 1 or 3, zone 2 hepatocytes are well positioned to avoid destruction. Altogether, these data suggested that the midlobular cells are capable of expansion, and ultimately regenerate the liver after common liver injuries.

IGFBP2+ zone 2 cells contribute to regeneration after partial hepatectomy

To assess the hepatocyte subpopulations that contribute to liver regrowth, we performed partial hepatectomy (PHx) on our lineage tracing mice. Compared to chemical injuries, PHx is not known to cause zone-specific damage. We used both the evening and fasting tamoxifen approaches to lineage trace after different extents of zone 2 labeling. To examine zone 2 hepatocyte contributions, we compared the Tomato labeling between liver tissue obtained from the initial surgical resection and the regenerated tissue 14 days after surgery (Figure 4A). Pre- and post-PHx livers showed a similar spatial distribution of Tomato+ cells (Figure 4B and Figure S5B). This unchanged zonal distribution revealed that there were contributions to regeneration from all three zones, in contrast to what was observed with pericentral or periportal injuries (Figure 3B, 3E). Indeed, it is known that most hepatocytes across the lobule proliferate after surgical resection [9]. To control for the variable labeling that occurs between individual mice, we further quantified the change in Tomato labeling frequency within each individual mouse, before and after surgery. This revealed a small but

Author Manuscript Author Manuscript Author Manuscript Author Manuscript

significant increase in Tomato labeling from 21.88 ± 11.25% to 26.27 ± 12.36% (Figure 4C). Similar results were also obtained from the fasting tamoxifen approach (27.29 ± 6.51% to 29.11 ± 8.41%) (Figure S5C, S5D). Previous studies showed that zone 1 and zone 2 hepatocytes together contribute more than zone 3 to liver regeneration after PHx [9,12], and our results showing a preferential contribution from zone 2 support those observations.

We next asked if hepatocytes from particular zones might serve as better donors in a hepatocyte transplant model. To do this, we transplanted zone 2 hepatocytes into immunodeficient *Fah*$^{-/-}$ mice (*Fah*$^{-/-}$; *Rag2*$^{-/-}$; *Il2rg*$^{-/-}$ [*FRG*]), a mouse model with tyrosinemia type I that can serve as a hepatocyte transplant recipient [13]. We used *Igfbp2-CreER* mice after fasting tamoxifen as a source of donor hepatocytes. To minimize technical bias from flow cytometry, we perfused *Igfbp2-CreER; LSL-tdTomato* livers and without sorting, directly transplanted one million viable hepatocytes into *FRG* recipients (Figure 4D). In this way, a mixture of primary hepatocytes that were Tomato+ (zone 2) and Tomato- (zone 1 and zone 3) populations could be transplanted into *FRG* recipients through splenic injection. The experiment was done with 7 *FRG* mice receiving donor #1 hepatocytes and 4 *FRG* mice receiving donor #2 hepatocytes. The left lateral lobes from each *Igfbp2-CreER* donor were removed before perfusion to ascertain the labeling efficiency of the midlobular population (Figure 4E). The recipient livers were harvested 7 weeks after transplantation and were immunostained for FAH to characterize the repopulation by all donor cells (Figure 4E). We observed patches of Tomato+ cells clustered together, indicating clonal expansion by donor derived cells. The transplanted Tomato+ cells, which were originally GS negative, were capable of adopting the appropriate expression pattern of the zone in which they repopulate, as evidenced by the emergence of GS and Tomato double positive cells after transplantation (Figure 4E). After repopulation, we calculated the percentage of zone 2 cells using the ratio of Tomato+ image area over FAH+ image area. There was a significant increase in Tomato percentage between donors (25.45 ± 0.92%) and recipients (28.85 ± 6.19%) in paired analysis (Figure 4F). These results suggested that zone 2 have a small advantage versus zone 1 and 3 hepatocytes in their contribution to liver repopulation after transplantation. If there was a rare stem cell population in zone 2 dominating repopulation, the Tomato+ area should have dramatically increased in comparison to the Tomato- area. The patches of Tomato+ cells suggested that clonal expansion occurred, but it was unlikely to have been caused by stem cell self-renewal since the Tomato negative cells also expanded. Both the PHx and *FRG* transplantation models demonstrated that most hepatocytes can proliferate after hepatic tissue loss.

Zone 2 hepatocytes contribute to pregnancy induced liver expansion

To meet the increased metabolic demands of pregnancy, the maternal liver dramatically increases in size [14]. It is unknown if there are differences in zonal contributions to pregnancy induced liver expansion. We utilized the *Igfbp2-CreER* line with the fasting tamoxifen approach to trace zone 2 hepatocytes during pregnancy. As a washout period, we waited four weeks after tamoxifen administration before mating was initiated. After delivery, offspring were separated from the mothers on the day of birth (P0) (Figure 5A). Remarkably, the body weight, liver weight, and liver to body weight ratios were all significantly increased in the pregnant cohort (Figure 5B,C). These data indicate that liver growth increases much

Author Manuscript Author Manuscript Author Manuscript Author Manuscript

more than would be expected if the liver was just enlarging to keep up with body weight changes. P0 mothers (41.81 ± 7.82%) showed an increase in Tomato labeling as compared to non-mated control females (34.37 ± 7.88%) (Figure 5D, 5E), indicating that zone 2 hepatocytes were contributing to pregnancy induced liver growth more than hepatocytes from other zones.

To trace an orthogonal zone Cre model, we utilized the *Gls2-CreER* line. *Gls2-CreER* mice label zone 1 hepatocytes surrounding the PV region (Figure 5F). The proportion of Tomato+ cells in *Gls2-CreER* declined during pregnancy (38.37 ± 1.26%) compared to non-mated control females (47.72 ± 1.93%) (Figure 5G). Given that there is overlapping Tomato labeling between *Igfbp2-CreER* and *Gls2-CreER* livers, we reason that the zone 2 cells located closer to the CV (not labeled by *Gls2-CreER*) contributed more toward liver growth during pregnancy.

Zonation changes during fasting

Surprisingly, the *Igfbp2-CreER* strain labeled a much larger number of midlobular hepatocytes after fasting (Figure 1). Because *Igfbp2* might not be the best or only marker for zone 2 cells, we needed to determine if other zone 2 markers were changing with fasting. While changes in the number of IGFBP2+ cells might suggest isolated changes in IGFBP2 itself without concomitant changes in other zonated gene expression programs, it is more likely that zonation domains shifted with fasting. If other zone 2 markers change, it would raise the larger question of how zonation might change between fed and fasted states. While the liver transcriptome is known to massively change during fasting [15], it is unknown how this occurs on the single cell level. As whole-body metabolism significantly changes during fasting, we speculated that zone specific metabolic functions may also be altered.

To investigate the impact of the fasted state on liver zonation and zone 2 cells, we performed single nuclear RNA sequencing (snRNA-seq) of livers from fed mice and those fasted for 24 hours. The UMAP plot of all liver cells showed a clear overlap of endothelial, hepatic stellate, and Kupffer cells between fed and fasted conditions (Figure 6A). In stark contrast, hepatocytes showed such large transcriptomic differences that fed and fasted hepatocytes were largely non-overlapping (Figure 6A). These data showed that fasting drives transcriptomic changes in hepatocytes but not in non-parenchymal cells (NPCs). Given the large differences between feeding and fasting, we analyzed the hepatocyte population separately from NPC populations (see details in the Methods). We were able to define three zones within fed and fasted conditions. Strikingly, we observed large increases in the frequency of zone 2 (37.0% to 53.2%) and zone 3 hepatocytes (from 11.1% to 19.7%), and a decrease of zone 1 hepatocytes (42.4% to 17.8%) (Figure 6B). To assess individual genes that are representative of zones, we compared the gene expression of zonal markers between fed and fasted states. We found increases in zone 2 (*Hamp*, *Igfbp2*) and zone 3 (*Oat*), and decreases in zone 1 (*Arg1*, *Gls2*) genes in fasting livers (Figure 6C). These results showed that hepatocyte gene expression in different zones changes dramatically after fasting. Altogether, the results showed that the *Igfbp2* expansion seen during fasting was not gene-specific, but instead influenced zonation more broadly.

Author Manuscript Author Manuscript Author Manuscript Author Manuscript

Next, we looked for the underlying basis of these zonal changes. Pathways that changed between fed and fasting states were similar in each of the three zones, indicating a coordinated change in metabolic programs throughout the lobule. We observed that oxidative phosphorylation, non-alcoholic fatty liver disease, fatty acid degradation, PPAR signaling pathway, and cholesterol metabolism genes increased with fasting (Figure S6B). Overall, all hepatocytes exhibited remarkable transcriptomic changes in the fasted state in order to maintain metabolic homeostasis. Therefore, the transcriptomic differences between zones was diminished. In addition, previously specialized metabolic functions that were more restricted to one zone were no longer restricted, indicating that zonal differences might be suppressed under fasting states. For example, in the fed liver, zone 1 hepatocytes with higher oxygen levels express genes involved in gluconeogenesis (e.g., *Pck1*) and have higher β-oxidation activity [7]. In the fasted liver, all zones were recruited to contribute towards gluconeogenesis and β-oxidation to release stored energy [16]. Examination of metabolic pathways in fed or fasting livers showed increased gluconeogenesis and fatty acid oxidation in the fasted state (Figure S6A), which could be an explanation for the decreased zone 1 population (Figure 6B) since other zones were also performing these metabolic functions.

Discussion

Although previous studies suggested that zone 2 hepatocytes are a major source for liver repopulation [6,8,9], there has been less direct evidence for the clonal expansion of this population, and few tools to track or genetically manipulate zone 2 cells. Our results showed that IGFBP2+ cells, which make up about 20–30% of the lobular hepatocyte population, increased in number during homeostasis and expanded more than cells from other zones after many types of injury. After hepatotoxic injuries occurring on either end of the lobule, we observed regeneration by IGFBP2+ cells into the injured area, further confirming that zone 2 hepatocytes are spatially positioned to compensate for cellular loss. Given the controversy in the liver field about the source of new hepatocytes, this additional quantitative evidence for zone 2 hepatocyte regeneration is needed.

There is likely to be additional heterogeneity among hepatocytes in zone 2. First, there is no clear definition of where boundaries are located between zones. Some studies distinguish zones based on expression of zonal markers (CDH1 for zone 1, GS for zone 3) [9]. We divide the lobule into three compartments based on distance along the PV-to-CV axis. IGFBP2+ cells are mostly in the middle third of the lobule. Based on our zonal definitions, there are some hepatocytes in zone 3 that are GS negative. In this way, we believe that not every hepatocyte between the GS+ and the CDH1+ domains should be considered zone 2.

Even based on our definition of zone 2 being IGFBP2 expressing, there is still heterogeneity within this population. First, the magnitude of expansion of the IGFBP2 population (~2 fold, from occupying 20.8% to 41.2%) is less than the HAMP2+ population (~3.7 fold, from 7.4% to 27.4%) during homeostasis over 1 year. Second, lineage tracing during pregnancy showed that IGFBP2 expressing midlobular cells expanded, while GLS2 expressing zone 1 cells declined in number. When comparing the occupancy and distribution of Tomato+ cells between these two models, there is considerable overlap in the labeled domains. *Gls2-CreER* labeled approximately half the diameter of the hepatic lobule surrounding the PV, which

Author Manuscript Author Manuscript Author Manuscript Author Manuscript

overlapped with approximately half of the IGFBP2+ zone 2 cells. This suggested that the zone 2 subpopulation closer to the CV (unlabeled by *Gls2-CreER*) might account for most of the expansion during pregnancy. This is consistent with our previous observation that GLS2+ cells make little contribution to the generation of new hepatocytes under homeostatic conditions[8]. Nevertheless, both Wei et. al., and this study came to the same conclusion that midlobular hepatocytes are more proliferative than other zone specific hepatocytes in multiple circumstances. Future studies using spatial transcriptomics may be able to investigate the subpopulations within zone 2 with greater cellular resolution. The interaction between hepatocytes and other non-parenchymal cells (e.g., endothelial cells, Kupffer cells, hepatic stellate cells, cholangiocytes, immune cells) may also contribute to the functional heterogeneity of the liver. Obtaining this information will help us further understand the mechanisms by which midlobular hepatocytes expand under distinct circumstances.

While it is known that heterogeneity of metabolic function is a central feature of hepatic zonation, how metabolic dysregulation changes zonation in physiological or pathological states is unknown. Hepatic gene expression changes dramatically in response to circadian rhythms and fasting/feeding states [15,17]. However, physiological processes that regulate zonation have not been elucidated. In this study, we characterized liver cell populations in normal and fasting states using lineage tracing and snRNA-seq. The results revealed an increase in hepatocytes expressing zone 2 and zone 3 genes at the expense of cells expressing zone 1 genes, which correlated with the observation of increased Tomato+ cells in fasted *Igfbp2-CreER* mice. It is still an open question whether zonation changes during fasting drive functional outcomes. Interestingly, fatty liver pathology also progresses in a zonated fashion. Are the health benefits of fasting caused in part by increased numbers of hepatocytes taking on zone 2/3 roles? Will the fasted liver become more susceptible to centrilobular damage due to an increase in zone 3 cells? Future work will need to determine how the zonation changes associated with fasting affect liver health and whole body metabolism.

Limitations of the Study

These zonation studies were based on mouse models and not on human tissues. It is unclear whether hepatic zonation is the same in mouse and human livers. The highly variable labeling efficiency of *Igfbp2-CreER* line may obscure some clonal expansion effects. Although the zone 1 and zone 3 compartments are likely changing during fasting, we have not examined the labeling pattern in fasted livers using other zonal *CreER* lines.

STAR Methods

RESOURCE AVAILABILITY

Lead Contact—Further information and requests for resources should be directed to the Lead Contact, Hao Zhu (hao.zhu@utsouthwestern.edu).

Materials Availability—Mouse lines generated in this study are available from the Lead Contact with a completed Materials Transfer Agreement.

Author Manuscript Author Manuscript Author Manuscript Author Manuscript

Data and code availability

- snRNA-seq data have been deposited at GEO and are publicly available (GSE228862).
- There is no original code in this paper.
- Any additional information required to reanalyze the data reported in this paper is available from the lead contact upon request.

EXPERIMENTAL MODELS AND STUDY PARTICIPANT DETAILS

Animals—The *Igfbp2-CreER* line was generated by CRISPR mouse engineering as described previously [8]. Briefly, a plasmid containing *IRES-CreERT2* flanked by homology arms from the 3' UTR of *Igfbp2* was used as a template to generate single stranded (ss)DNAs. SsDNA, CAS9 protein, and sgRNA(s) were co-injected into mouse zygotes. All mice were maintained in a specific pathogen free (SPF) facility and handled in accordance with the guidelines of the Institutional Animal Care and Use Committee (IACUC) of UTSW. Tamoxifen (Sigma-Aldrich #T5648) was dissolved in corn oil and given at a dose of 100 mg/kg into 6-week-old mice as described in Figure 1. *FRG* mice were purchased from Yecuris (#10–0001) and maintained on 7.5 μg/mL nitisinone (NTBC, Yecuris #20–0027) water until transplantation. Homeostasis tracing (Figure 1 and Figure 2) and PHx (Figure 4A–4C) were performed on both male and female mice. Chemical injury (Figure 3), FRG transplantation (Figure 4D–4F) and snRNA-seq (Figure 6) were performed on male mice. The pregnancy experiment (Figure 5) employed female mice. All experiments were done in an age and sex matched fashion. The sex and age status of the animals used were specified in the legends.

METHOD DETAILS

Chemical Injury Experiments—CCl_4 (Sigma Aldrich #289116) was diluted 1:10 in corn oil and injected one time IP at a dose of 0.5 ml/kg of mouse. Acetaminophen, or APAP (Sigma Aldrich #A7085), was dissolved in warm saline and injected one time IP at 300 mg/kg of mouse. The livers were harvested 2 weeks after injection. DDC was mixed into TestDiet at 0.1% concentration and the mice were fed for 4 weeks starting 2 weeks after tamoxifen.

Partial Hepatectomy—Two thirds of the liver was surgically removed in the standard fashion as described previously [18]. The left lateral lobe and the median lobe were removed, and used as pre-surgical samples for Tomato analysis. The regenerated livers were harvested 2 weeks after surgery. Pre- and post-surgical samples were compared for the same mice using paired Student's t-tests.

Immunofluorescence—Livers were fixed overnight in 4% paraformaldehyde (PFA; Alfa Aesar #J19943K2) at 4°C. For frozen sectioning, the livers were further dehydrated in 30% sucrose overnight at 4°C. Tissues were frozen sectioned at a thickness of 16 μm, washed with PBST three times and blocked in 5% BSA with 0.25% Triton X-100 at room temperature for 1 hour. The slides were incubated with GS antibody (Abcam #ab49873; 1:1000) or FAH antibody (Yecuris #20–0042; 1:500) in the blocking solution at 4°C

Author Manuscript Author Manuscript Author Manuscript Author Manuscript

overnight. After washing three times with PBST, slides were incubated with Alexa Fluor 488 goat anti-rabbit IgG antibody (Life technologies #A-11008) at a 1:200 dilution and Hoechst 33342 (Life technologies #H3570) at 1:1000 dilution in the blocking solution at room temperature for 1 hour. For IGFBP2 and E-cadherin staining, fixed tissues were embedded in paraffin and sectioned. The paraffin-sectioned slides were deparaffinized in xylene and rehydrated in 100%, 90%, 80%, 70%, 50%, and 30% ethanol and deionized water. Citra Plus Antigen Retrieval (Fisher #NC9755543) with 0.05% Tween 20 was used for heat-induced antigen retrieval by microwaving. The slides were blocked in 5% BSA with 0.25% Triton X-100 at room temperature for 1 hour, and then the staining was performed as described above. For paraffin slides, the following antibodies were used: E-cadherin (Bio-Techne #AF748), IGFBP2 (Abcam #ab188200), RFP (Rockland #600–401-379), RFP (Life technologies #MA5–15257), Alexa Fluor 488 donkey anti-goat IgG antibody (Life technologies #A-11055), Alexa Fluor 594 donkey anti-rabbit IgG antibody (Life technologies #A-21207), Alexa Fluor 488 goat anti-mouse IgG1 antibody (Life technologies #A-21121). Whole slides were imaged using an Axioscan slide scanner and processed using Zen 2.6 software from Zeiss.

Image quantification—ImageJ was used to quantify the percentage of Tomato+ areas as described previously[8]. In the lineage tracing images, we used frozen sections to preserve the Tomato signal directly from the labeled cells. To distinguish CVs from PVs, we used GS immunofluorescence with a 488 secondary antibody. Since the liver tissue exhibits autofluorescence, especially in the green channel, we found that this signal can define the whole tissue area when you saturate the signal. Therefore, we used the green channel to measure the total tissue area while excluding the blank areas that correspond to larger vascular structures. Briefly, the composite RBG images were separated into three channels. We then adjusted the threshold to saturate the Tomato signal in the red channel and to cover all the tissue areas in the green channel. Because there is variability across a liver section, Tomato+ areas were calculated using whole slide images rather than individual cropped images. Each mouse in the study had one associated whole slide image.

EdU Proliferation Assay—Both the control (*LSL-tdTomato* heterozygous) and *Igfbp2-CreER* (*Igfbp2-CreER; LSL-tdTomato* heterozygous) mice were given tamoxifen at 6 weeks of age. Two weeks after tamoxifen, water containing 1 mg/mL EdU (Carbosynth #NE08701) was provided to males for 14 days. The livers were then harvested and frozen-sectioned. The Click-iT EdU Alexa Fluor 488 Imaging Kit (Life Technologies #C10337) was used to detect the EdU signal. Following EdU staining, GS and Alexa Fluor 647 goat anti-rabbit IgG antibodies (Life technologies #A-21244) were used to mark hepatocytes around CVs. The zonal position indices (P.I.) for EdU+ hepatocytes were determined as previously described [4]. We only analyzed proliferating hepatocytes, which have large and round nuclei in comparison to the nuclei of non-parenchymal cells. The distance of an EdU+ nuclei to the closest CV (x) and closest PV (y), and the distance between the CV and PV (z) were measured. The position index (P.I.) was calculated using this formula: $P.I. = (x^2 + z^2 - y^2)/(2z^2)$.

Author Manuscript Author Manuscript Author Manuscript Author Manuscript

Hepatocyte isolation and transplantation—Primary hepatocytes were isolated by the 2-step collagenase perfusion through the inferior vena cava. Mice were perfused with Liver Perfusion Medium (Gibco #17701038) followed by Liver Digest Medium (Gibco #17703034). The liver cell suspension was filtered through a 70 μM strainer. Equal amounts of Hepatocyte Wash Medium (Gibco #17704024) was added to the liver cell suspension and centrifuged at 50 g for 5 minutes to collect hepatocytes. After two washes, the primary hepatocytes were counted and diluted in Hepatocyte Wash Medium. Finally, 1×10^6 cells were resuspended in 200 μL and transplanted into *FRG* mice through splenic injection. NTBC water was withdrawn immediately after injection.

Single nuclear RNA sequencing (snRNA-seq)—6 week old C57BL/6 mice were purchased from Jackson Laboratory and maintained until 8 weeks of age. Mice were fasted for 24 hours before hepatocyte isolation. Littermates with ad libitum feeding were collected at the same time. After washes, primary hepatocytes were resuspended in GBSS (Sigma Aldrich #G9779) with 0.7% CHAPS (Sigma Aldrich #C5070) and 0.2U/μL RNase inhibitor (Roche Diagnostics #3335399001), and kept on ice for 5 min. The samples were centrifuged at 500g for 5 minutes and further washed twice using PBS with 1% BSA and 0.2U/μL RNase inhibitor. The nuclear extraction efficiency was determined with trypan blue under a microscope. The isolated nuclei were resuspended in the wash buffer to around 1×10^6 nuclei/mL. Single nuclei libraries were prepared using the 10x Genomics Chromium Single Cell 3' Reagents Kit v3.1 according to the manufacturer's protocol. For each sample, two biological replicates (n = 2 mice) were collected and combined. About 8000 nuclei were mixed with reverse transcription master mix and loaded onto Next GEM Chip-G to target ~5,000 nuclei after recovery. Libraries were sequenced using 150 bp paired-end Illumina NextSeq500 system at the UTSW Children's Research Institute Sequencing Facility.

SnRNA-seq analysis—10x scRNA-seq data was preprocessed using the Cell Ranger software (5.0.0). Mouse genome assembly GRCm38 was used for the alignment step. The "mkfastq", "count," and 'aggr' commands were used to process the 10x scRNA-seq output into a cell by gene expression count matrix. Default parameters were used in the 'mkfastq' and 'aggr' commands and intronic reads were kept in the 'count' command. scRNA-seq data analysis was performed using the Scanpy package in Python [19]. For quality control, genes expressed in fewer than 3 cells were removed from further analysis. Cells expressing less than 500 genes or with a high (>= 0.1) mitochondrial genome transcript ratio were removed from further analysis. For downstream analysis, we used count per million normalizations (CPM) to control for library size differences in cells. A Python implementation of the Harmony algorithm (https://github.com/immunogenomics/harmony) was used to reduce batch effects in data. After normalization, we used the 'pp.highly_variable_genes' command in Scanpy to find highly variable genes across all cells using default parameters except for "min_mean = 0.01" and "min_disp=0.5". The data were then z-score normalized for each gene across all cells. We then used the 'tl.pca', the 'pp.neighbors (n_pcs=25)' and the 'tl.leiden (resolution = 0.75)' command in Scanpy to partition the single cells into clusters. Differential expression analysis was performed using the Wilcoxon Rank Sum test implemented in the 'tl.rank_genes_groups' function.

Author Manuscript Author Manuscript Author Manuscript Author Manuscript

Functional enrichment analysis and GSEA analysis were performed using the 'GSEApy' Python package [https://github.com/zqfang/GSEApy].

QUANTIFICATION AND STATISTICAL ANALYSIS

The data in most panels reflect multiple experiments performed on different days using mice derived from different litters. Variation is indicated in the plots using standard error presented as mean ± SEM. In the text, variation is indicated using standard deviation presented as mean ± SD. Two-tailed Student's t-tests (two-sample equal variance) were used to test the significance of differences between two groups unless otherwise specified. In all figures, statistical significance is displayed as * ($p < 0.05$), ** ($p < 0.01$), *** ($p < 0.001$), ****($p < 0.0001$). In the PHx experiment, paired Student's t-tests were used to test the significance comparing the excised and regenerated liver lobes. In the *FRG* transplantation experiments, each donor's Tomato percentage was used as individual data points and the statistical analysis was performed using the paired Student's t-test. The statistical significance is displayed as # ($p < 0.05$), ## ($p < 0.01$) in the paired analysis. In all experiments, mice were not excluded from analysis after the experiment was initiated, unless the mice died. Image analysis for quantification was blinded.

Supplementary Material

Refer to Web version on PubMed Central for supplementary material.

Acknowledgements

We would like to thank D. Ramirez (UTSW Whole Brain Microscopy Facility) for whole liver imaging; C. Lewis (UTSW Tissue Procurement Service) for histopathology; J. Xu and Y. J. Kim (CRI Sequencing Core) for sequencing; T.W. is supported by NIH (R01CA258584). H.Z. is supported by the Pollack Foundation, the NIH R01 grants (AA028791, DK125396), a Simmons Comprehensive Cancer Center Cancer & Obesity Translational Pilot Award, and the Emerging Leader Award from the Mark Foundation For Cancer Research (#21-003-ELA).

H.Z. has a sponsored research agreement with Alnylam Pharmaceuticals, consults for Flagship Pioneering and Chroma Medicines, and serves on the SAB of Ubiquitix.

References

1. Furuyama K, Kawaguchi Y, Akiyama H, Horiguchi M, Kodama S, Kuhara T, Hosokawa S, Elbahrawy A, Soeda T, Koizumi M, et al. (2011). Continuous cell supply from a Sox9-expressing progenitor zone in adult liver, exocrine pancreas and intestine. Nat. Genet. 43, 34–41. 10.1038/ng.722. [PubMed: 21113154]
2. Font-Burgada J, Shalapour S, Ramaswamy S, Hsueh B, Rossell D, Umemura A, Taniguchi K, Nakagawa H, Valasek MA, Ye L, et al. (2015). Hybrid Periportal Hepatocytes Regenerate the Injured Liver without Giving Rise to Cancer. Cell 162, 766–779. 10.1016/j.cell.2015.07.026. [PubMed: 26276631]
3. Wang B, Zhao L, Fish M, Logan CY, and Nusse R (2015). Self-renewing diploid Axin2(+) cells fuel homeostatic renewal of the liver. Nature 524, 180–185. 10.1038/nature14863. [PubMed: 26245375]
4. Lin S, Nascimento EM, Gajera CR, Chen L, Neuhöfer P, Garbuzov A, Wang S, and Artandi SE (2018). Distributed hepatocytes expressing telomerase repopulate the liver in homeostasis and injury. Nature 556, 244–248. 10.1038/s41586-018-0004-7. [PubMed: 29618815]
5. Sun T, Pikiolek M, Orsini V, Bergling S, Holwerda S, Morelli L, Hoppe PS, Planas-Paz L, Yang Y, Ruffner H, et al. (2020). AXIN2+ pericentral hepatocytes have limited contributions to liver homeostasis and regeneration. Cell Stem Cell 26, 97–107.e6. 10.1016/j.stem.2019.10.011. [PubMed: 31866224]

Author Manuscript Author Manuscript Author Manuscript Author Manuscript

6. Chen F, Jimenez RJ, Sharma K, Luu HY, Hsu BY, Ravindranathan A, Stohr BA, and Willenbring H (2020). Broad distribution of hepatocyte proliferation in liver homeostasis and regeneration. Cell Stem Cell 26, 27–33.e4. 10.1016/j.stem.2019.11.001. [PubMed: 31866223]
7. Ben-Moshe S, and Itzkovitz S (2019). Spatial heterogeneity in the mammalian liver. Nat. Rev. Gastroenterol. Hepatol. 16, 395–410. 10.1038/s41575-019-0134-x. [PubMed: 30936469]
8. Wei Y, Wang YG, Jia Y, Li L, Yoon J, Zhang S, Wang Z, Zhang Y, Zhu M, Sharma T, et al. (2021). Liver homeostasis is maintained by midlobular zone 2 hepatocytes. Science 371. 10.1126/science.abb1625.
9. He L, Pu W, Liu X, Zhang Z, Han M, Li Y, Huang X, Han X, Li Y, Liu K, et al. (2021). Proliferation tracing reveals regional hepatocyte generation in liver homeostasis and repair. Science 371. 10.1126/science.abc4346.
10. Tseng LY, Ooi GT, Brown AL, Straus DS, and Rechler MM (1992). Transcription of the insulin-like growth factor-binding protein-2 gene is increased in neonatal and fasted adult rat liver. Mol. Endocrinol. 6, 1195–1201. 10.1210/mend.6.8.1383692. [PubMed: 1383692]
11. Fickert P, Stöger U, Fuchsbichler A, Moustafa T, Marschall H-U, Weiglein AH, Tsybrovskyy O, Jaeschke H, Zatloukal K, Denk H, et al. (2007). A new xenobiotic-induced mouse model of sclerosing cholangitis and biliary fibrosis. Am. J. Pathol. 171, 525–536. 10.2353/ajpath.2007.061133. [PubMed: 17600122]
12. Chembazhi UV, Bangru S, Hernaez M, and Kalsotra A (2021). Cellular plasticity balances the metabolic and proliferation dynamics of a regenerating liver. Genome Res. 31, 576–591. 10.1101/gr.267013.120. [PubMed: 33649154]
13. Azuma H, Paulk N, Ranade A, Dorrell C, Al-Dhalimy M, Ellis E, Strom S, Kay MA, Finegold M, and Grompe M (2007). Robust expansion of human hepatocytes in Fah−/−/Rag2−/−/Il2rg−/− mice. Nat. Biotechnol. 25, 903–910. 10.1038/nbt1326. [PubMed: 17664939]
14. Dai G, Bustamante JJ, Zou Y, Myronovych A, Bao Q, Kumar S, and Soares MJ (2011). Maternal hepatic growth response to pregnancy in the mouse. Exp Biol Med (Maywood) 236, 1322–1332. 10.1258/ebm.2011.011076. [PubMed: 21969712]
15. Sokolović M, Sokolović A, Wehkamp D, Ver Loren van Themaat E, de Waart DR, Gilhuijs-Pederson LA, Nikolsky Y, van Kampen AHC, Hakvoort TBM, and Lamers WH (2008). The transcriptomic signature of fasting murine liver. BMC Genomics 9, 528. 10.1186/1471-2164-9-528. [PubMed: 18990241]
16. Rui L (2014). Energy metabolism in the liver. Compr. Physiol. 4, 177–197. 10.1002/cphy.c130024. [PubMed: 24692138]
17. Bookout AL, de Groot MHM, Owen BM, Lee S, Gautron L, Lawrence HL, Ding X, Elmquist JK, Takahashi JS, Mangelsdorf DJ, et al. (2013). FGF21 regulates metabolism and circadian behavior by acting on the nervous system. Nat. Med. 19, 1147–1152. 10.1038/nm.3249. [PubMed: 23933984]
18. Mitchell C, and Willenbring H (2008). A reproducible and well-tolerated method for 2/3 partial hepatectomy in mice. Nat. Protoc. 3, 1167–1170. 10.1038/nprot.2008.80. [PubMed: 18600221]
19. Wolf FA, Angerer P, and Theis FJ (2018). SCANPY: large-scale single-cell gene expression data analysis. Genome Biol. 19, 15. 10.1186/s13059-017-1382-0. [PubMed: 29409532]

Author Manuscript Author Manuscript Author Manuscript Author Manuscript

Highlights

- *Igfbp2-CreER* mice allow for genetic manipulation in midlobular zone 2 hepatocytes.
- Lineage tracing showed that midlobular hepatocytes proliferate during homeostasis.
- Zone 2 cells were protected from common liver injuries and replaced lost hepatocytes.
- Fasting induced significant changes in liver zonation.

Author Manuscript Author Manuscript Author Manuscript Author Manuscript

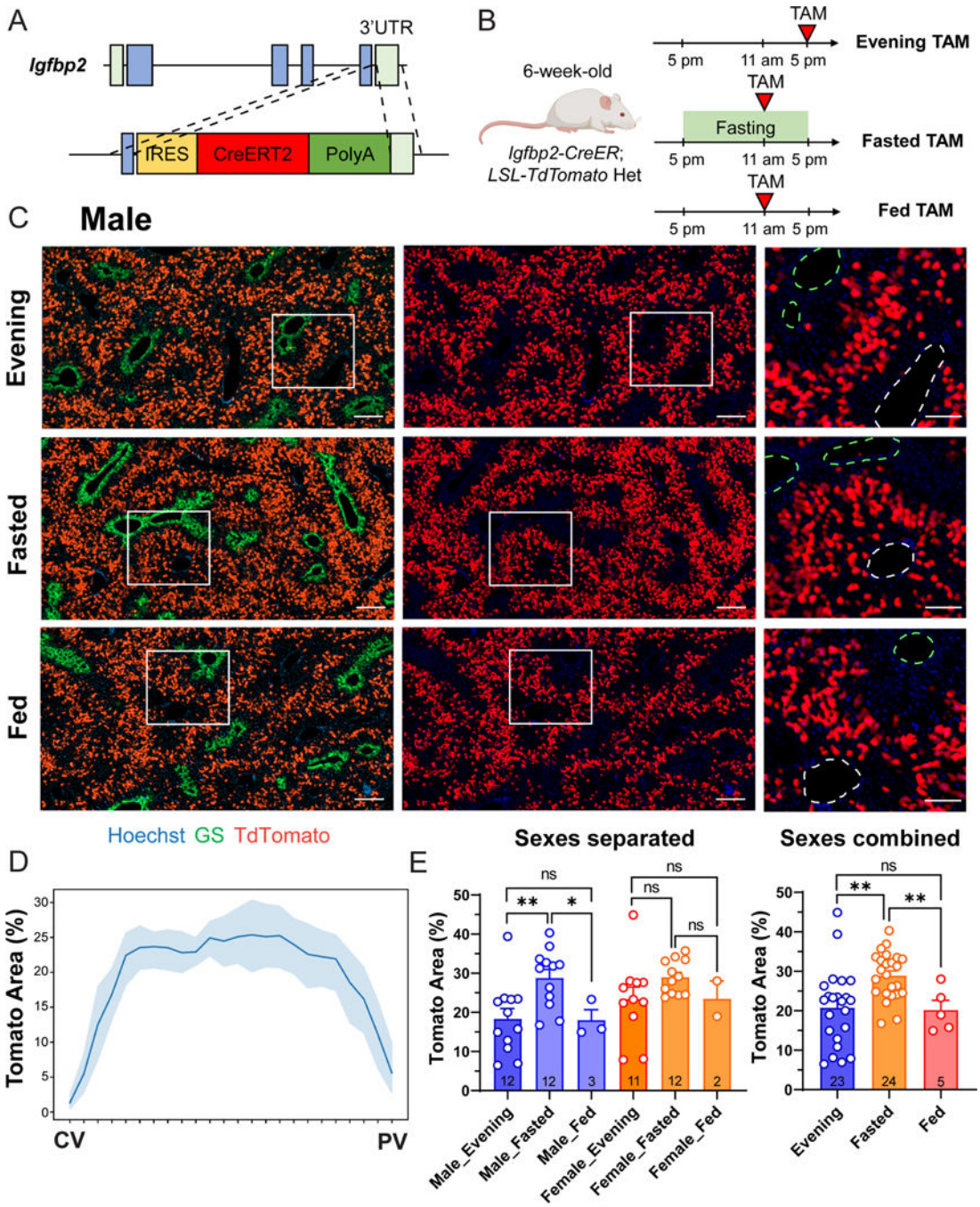

Figure 1. The *Igfbp2-CreER* strain labels zone 2 hepatocytes in a nutrient-dependent manner.

A. Schema of the homology directed repair (HDR) construct used to generate the *Igfbp2-CreER* strain.

B. Schema of three different tamoxifen administration approaches.

C. Representative images of male *Igfbp2-CreER; tdTomato* het mouse livers two weeks after tamoxifen given at 100mg/kg intraperitoneally using different approaches. In magnified images, the green dashed circles represent CVs (marked by GS), and the white dashed

Author Manuscript Author Manuscript Author Manuscript Author Manuscript

circles represent PVs. Scale bar = 200 μm for cropped images and 100 μm for magnified images.

D. The percent area labeled in *Igfbp2-CreER* mice given evening tamoxifen.

E. The quantification of the Tomato+ areas of the three tamoxifen approaches. The right panel combines the data points from the two sexes shown in the left panel. The data points of evening and fasting tamoxifen are the same as in the 2-week timepoint in Figure 2C and S4D (n = 23, 24 and 5 mice for evening, fasted, and fed groups respectively).

All data in this figure are presented as mean ± SEM. Significance is displayed as $p < 0.05$ (*), $p < 0.01$ (**), $p < 0.001$(***), and $p < 0.0001$ (****).

Author Manuscript Author Manuscript Author Manuscript Author Manuscript

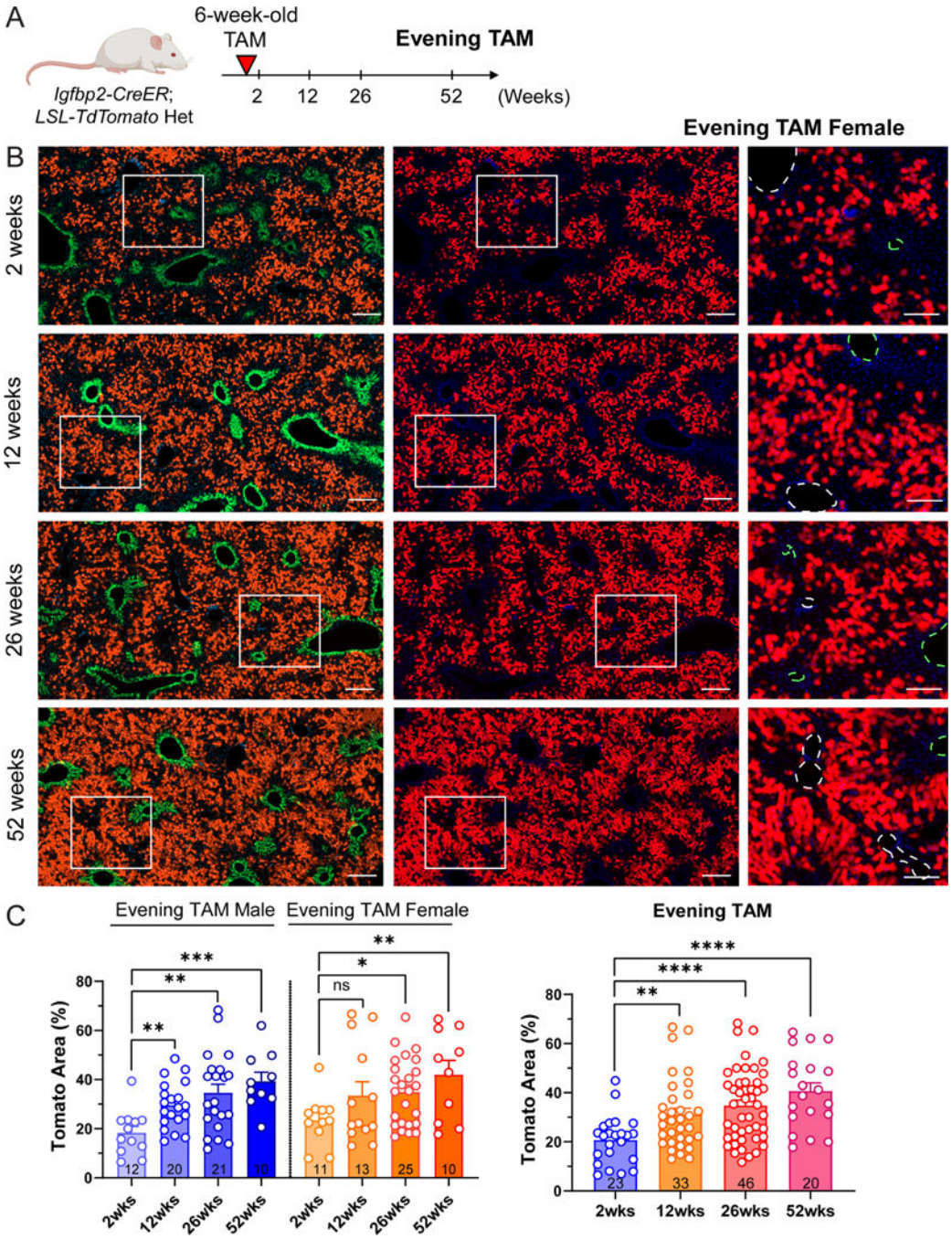

Figure 2. Zone 2 hepatocytes give rise to new hepatocytes during normal homeostasis.

A. Schema of evening tamoxifen lineage tracing experiment under normal homeostasis.

B. Representative images of female evening tamoxifen lineage tracing over 2, 12, 26 and 52 weeks under homeostatic conditions. Scale bar = 200 μm for cropped images and 100 μm for magnified images. Slides were stained for GS (green). The green dashed circles represent CVs (marked by GS), and the white dashed circles represent PVs.

Author Manuscript Author Manuscript Author Manuscript Author Manuscript

C. Quantification of the Tomato area from **B**. The right panel combines the data points from two sexes shown in the left panel. The 2-week data points are the same as the evening timepoints in Figure 1E (n = 23, 33, 46 and 20 mice for 2, 12, 26 and 52 weeks).
All data in this figure are presented as mean ± SEM. Significance is displayed as $p < 0.05$ (*), $p < 0.01$ (**), $p < 0.001$(***), and $p < 0.0001$ (****).

Author Manuscript Author Manuscript Author Manuscript Author Manuscript

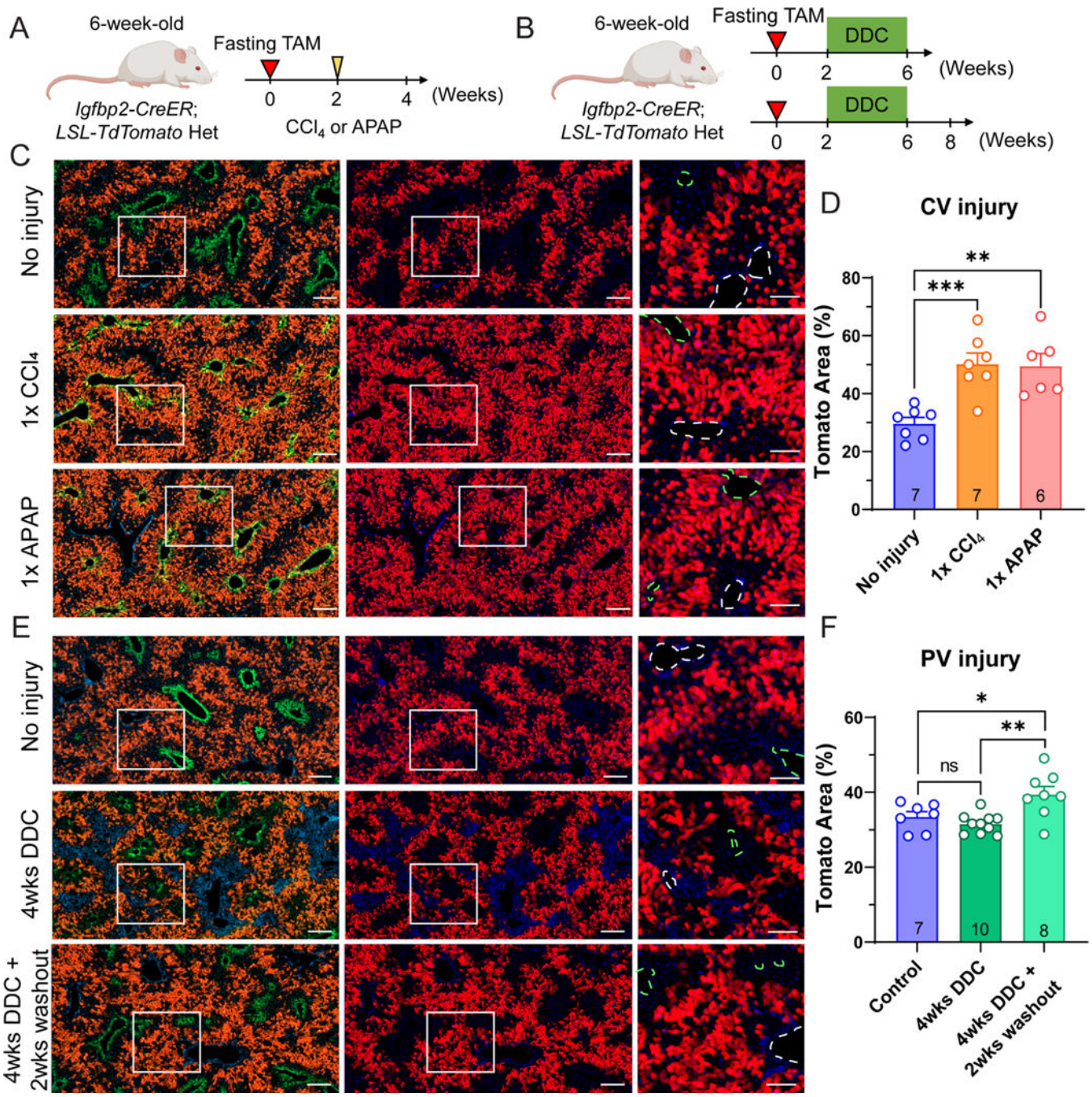

Figure 3. IGFBP2+ zone 2 cells regenerate after both pericentral and periportal injuries.

A. Schema of fasting tamoxifen males challenged with CCl_4 or APAP.

B. Schema of fasting tamoxifen males given 4 weeks of DDC diet.

C. Representative images of fasting tamoxifen treated males without injury or two weeks after CCl_4 or APAP injury. Scale bar = 200 μm for cropped images and 100 μm for magnified images. Slides were stained for GS (green). The green dashed circles represent CVs (marked by GS), and the white dashed circles represent PVs.

Author Manuscript Author Manuscript Author Manuscript Author Manuscript

D. Quantification of the Tomato area from **C** (n = 7, 7 and 6 mice for no injury, CCl_4 and APAP, respectively).

E. Representative images of fasting tamoxifen male without injury, after 4 weeks of DDC feeding, or after 4 weeks DDC plus a 2 week washout period with normal chow. Scale bar = 200 μm for cropped images and 100 μm for magnified images. Slides were stained for GS (green). The green dashed circles represent CVs (marked by GS), and white dashed circles represent PVs.

F. Quantification of the Tomato area from **E** (n = 7, 10, and 8 mice for control diet, 4 weeks of DDC, and 4 weeks of DDC + 2 weeks of washout).

All data in this figure are presented as mean ± SEM. Significance is displayed as $p < 0.05$ (*), $p < 0.01$ (**), $p < 0.001$(***), and $p < 0.0001$ (****).

Author Manuscript Author Manuscript Author Manuscript Author Manuscript

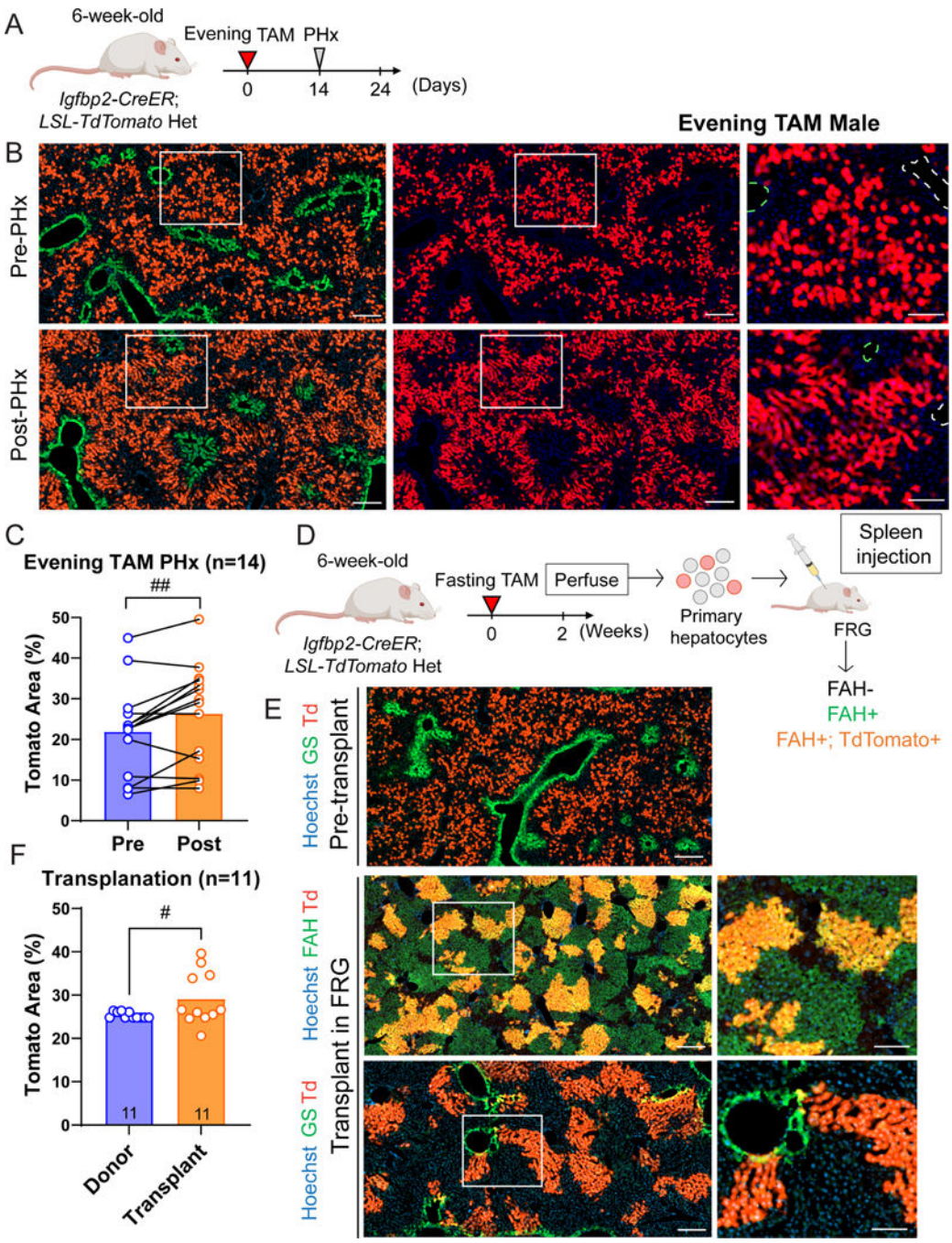

Figure 4. Zone 2 hepatocytes labeled by *Igfbp2-CreER* contribute to liver regeneration and repopulation.

A. Schema of the *Igfbp2-CreER* lineage tracing experiment in the context of PHx.

B. Representative images of evening tamoxifen male livers pre- and post-PHx. Scale bar = 200 μm for cropped images and 100 μm for magnified images. Slides were stained for GS (green). The green dashed circles represent CVs (marked by GS), and the white dashed circles represent PVs.

Author Manuscript Author Manuscript Author Manuscript Author Manuscript

C. Quantification of the Tomato area from **B**. Significance was assessed by paired t-tests (n = 14 mice).

D. Schema of primary hepatocyte transplantation from *Igfbp2-CreER* mice into *FRG* mice.

E. Representative images of pre-transplant donor livers and the post-transplant repopulated livers. Scale bar = 200 μm for cropped images and 100 μm for magnified images. In the donor livers, slides were stained for GS (green). In the transplanted *FRG* livers, slides were either stained for FAH (upper) or GS (lower).

F. Quantification of the Tomato area from **E**. The percentage was quantified by taking the ratio of the Tomato area over the FAH area in the transplanted livers (n = 11 and 11 mice for the donors and recipients). The donor Tomato percentages were plotted as 11 individual data points coming from 2 donor mice.

All data in this figure are presented as mean ± SEM. The statistical significance is displayed as # ($p < 0.05$), ## ($p < 0.01$) in the paired analysis.

Author Manuscript Author Manuscript Author Manuscript Author Manuscript

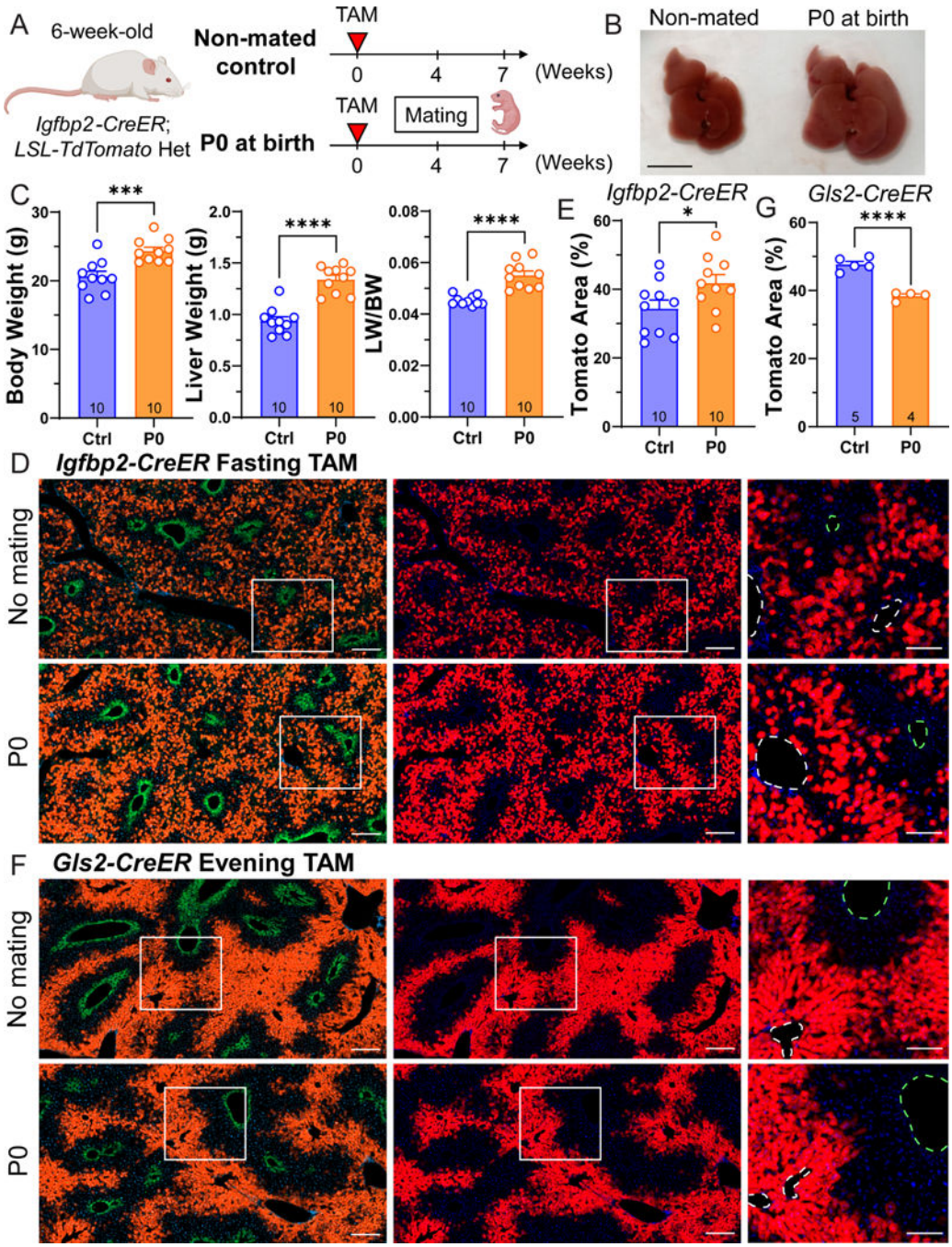

Figure 5. Zone 2 cells contribute to liver expansion during pregnancy

A. Schema of the pregnancy lineage tracing experiment. *Igfbp2-CreER* mice were given tamoxifen at 6 weeks of age, and mated 4 weeks afterwards. The livers were harvested when the pups were born (P0) in the pregnancy group.

B. Gross images of livers from control and pregnant mice. Scale bar, 1 cm.

C. Body weight, liver weight, and liver-to-body weight ratios of non-mated controls (Ctrl) and the pregnant group collected at P0 (n = 10 and 10 for control and pregnant mice).

Author Manuscript Author Manuscript Author Manuscript Author Manuscript

D. Representative images of control and pregnant livers from *Igfbp2-CreER* mice. Scale bar = 200 μm for cropped images and 100 μm for magnified images. Slides were stained for GS (green). The green dashed circles represent CVs (marked by GS), and the white dashed circles represent PVs.

E. Quantification of the Tomato area from **D** (n = 10 and 10 for control and pregnant mice).

F. Representative images of control and pregnant livers from *Gls2-CreER* mice. Scale bar = 200 μm for cropped images and 100 μm for magnified images. Slides were stained for GS (green). The green dashed circles represent CVs (marked by GS), and the white dashed circles represent PVs.

G. Quantification of the Tomato area from **F** (n = 5 control and 4 pregnant mice).

All data in this figure are presented as mean ± SEM. Significance is displayed as $p < 0.05$ (*), $p < 0.01$ (**), $p < 0.001$(***), and $p < 0.0001$ (****).

Author Manuscript Author Manuscript Author Manuscript Author Manuscript

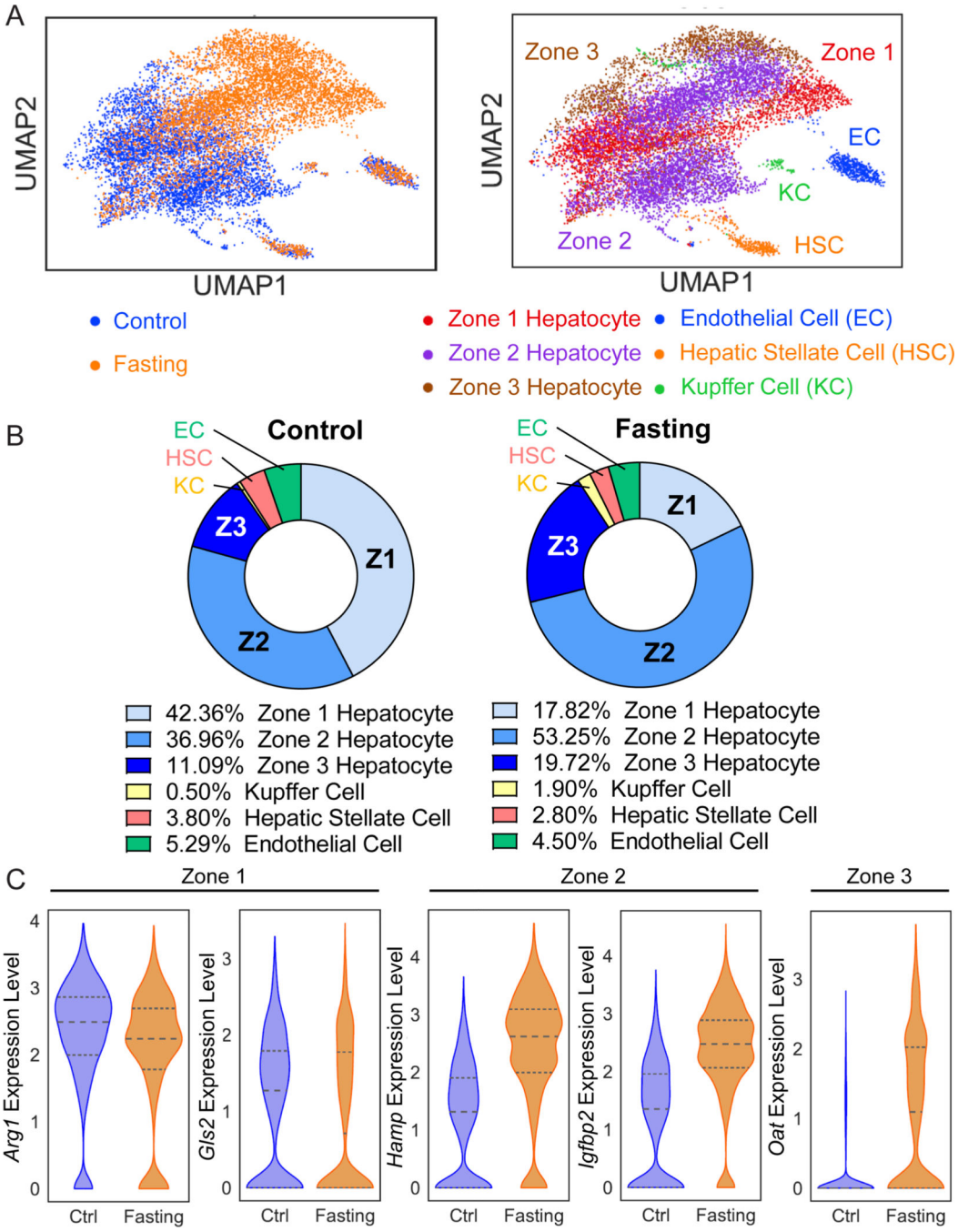

Figure 6. snRNA-seq revealed significant transcriptomic and zonation changes in the fasted liver.

A. Uniform Manifold Approximation and Projection (UMAP) plots represent the clustering of two samples (left panel) and cell populations (right panel). Nuclei from two fed livers were combined and two fasted livers were combined for the snRNA-seq experiment.

B. This pie chart indicates the proportions of each cell population in fed (left panel) and fasted livers (right panel).

Author Manuscript Author Manuscript Author Manuscript Author Manuscript

C. Gene expression of zonal markers (Zone 1: *Arg1*, *Gls2*; Zone 2: *Hamp*, *Igfbp2*; Zone 3: *Oat*) in fed and fasted livers.

Author Manuscript Author Manuscript Author Manuscript Author Manuscript

Key resources table

REAGENT or RESOURCE	SOURCE	IDENTIFIER
Antibodies		
Rabbit polyclonal anti-GS	Abcam	Cat#49873; RRID: AB_880241
Rabbit polyclonal anti-FAH	Yecuris	Cat#20–0034
Goat polyclonal anti-E-Cadherin	Bio-Techne	Cat#AF748; RRID: AB_355568
Rabbit monoclonal anti-IGFBP2	Abcam	Cat#188200
Rabbit polyclonal anti-RFP	Rockland	Cat#600–401-379; RRID: AB_2209751
Mouse monoclonal anti-RFP	Life technologies	Cat#MA5–15257; RRID: AB_10999796
Goat anti Rabbit IgG, Alexa Fluor 488 conjugated	Life technologies	Cat#A-11008; RRID: AB_143165
Donkey anti Goat IgG, Alexa Fluor 488 conjugated	Life technologies	Cat#A-11055; RRID: AB_2534102
Donkey anti Rabbit IgG, Alexa Fluor 594 conjugated	Life technologies	Cat#A-21207; RRID: AB_141637
Goat anti Mouse IgG1, Alexa Fluor 488 conjugated	Life technologies	Cat#A-21121; RRID: AB_2535764
Goat anti Rabbit IgG, Alexa Fluor 647 conjugated	Life technologies	Cat#A-21244; RRID: AB_2535812
Bacterial and virus strains		
Biological samples		
Chemicals, peptides, and recombinant proteins		
Tamoxifen	Sigma-Aldrich	Cat#T5648
CuRx Nitisinone (NTBC)	Yecuris	Cat#20–0027
5-ethynyl-2’-deoxyuridine (EdU)	Carbosynth	Cat#NE08701
Carbon tetrachloride (CCl_4)	Sigma Aldrich	Cat#289116
Acetaminophen	Sigma Aldrich	Cat#A7085
4% Paraformaldehyde Solution in PBS	Alfa Aesar	Cat#J19943K2
Hoechst 33342	Life technologies	Cat#H3570
Citra Plus Antigen Retrieval	Fisher	Cat#NC9755543
Gey’s Balanced Salt Solution	Sigma Aldrich	Cat#G9779
CHAPS	Sigma Aldrich	Cat#C5070
RNase inhibitor	Roche Diagnostics	Cat#3335399001
Hoechst 33342	Life technologies	Cat#H3570
Critical commercial assays		
Click-iT EdU Alexa Fluor 488 Imaging Kit	Life Technologies	Cat#C10337
Liver Perfusion Medium	Gibco	Cat#17701038
Liver Digest Medium	Gibco	Cat#17703034
Hepatocyte Wash Medium	Gibco	Cat#17704024
Chromium Single Cell 3’ Reagents Kit v3.1	10x Genomics	Cat#PN-1000269
Chromium Next GEM Chip G Single Cell Kit	10x Genomics	Cat#PN-1000127
Dual Index Kit TT Set A	10x Genomics	Cat#PN-1000215
Qubit dsDNA BR Assay Kit	Invitrogen	Cat #Q32850
Deposited data		

Author Manuscript Author Manuscript Author Manuscript Author Manuscript

REAGENT or RESOURCE	SOURCE	IDENTIFIER
Raw and analyzed snRNA-seq data	This paper	GEO: GSE228862
Experimental models: Cell lines		
Experimental models: Organisms/strains		
Mouse: C57BL/6J	The Jackson Laboratories	JAX: 000664
Mouse: *Rag1* KO; *Fah* KO; *Il2rg* KO on C57BI/6	Yecuris	Cat #10–0001
Mouse: *Igfbp2-CreER*	This paper	N/A
Oligonucleotides		
Recombinant DNA		
Software and algorithms		
Cell Ranger software	10x Genomics	https://support.10xgenomics.com/single-cell-gene-expression/software/pipelines/latest/what-is-cell-ranger
Scanpy package	Wolf et al., 2018	https://github.com/theislab/Scanpy
GSEApy package	Fang et al., 2023	https://github.com/zqfang/GSEApy
Other		